HHS Public Access

Author manuscript

*J Med Chem*. Author manuscript; available in PMC 2016 August 03.

Published in final edited form as:

*J Med Chem*. 2015 August 13; 58(15): 5770–5780. doi:10.1021/acs.jmedchem.5b00356.

# Biological Efficacy and Toxicity of Diamidines in Myotonic Dystrophy Type 1 Models

**Ruth B. Siboni**[a], **Micah J. Bodner**[b], **Muhammad M. Khalifa**[b], **Aaron G. Docter**[b], **Jessica Y. Choi**[b], **Masayuki Nakamori**[c], **Michael M. Haley**[b], and **J. Andrew Berglund**[a,b,*]

[a]Institute of Molecular Biology, University of Oregon, Eugene, OR 97403

[b]Department of Chemistry and Biochemistry, University of Oregon, Eugene, OR 97403

[c]Department of Neurology, University of Osaka Graduate School of Medicine, Osaka, Japan

## Abstract

Myotonic Dystrophy type 1 (DM1) is a disease characterized by errors in alternative splicing, or "mis-splicing". The causative agent of mis-splicing in DM1 is an inherited CTG repeat expansion located in the 3′ untranslated region of the DM protein kinase gene. When transcribed, CUG repeat expansion RNA sequester MBNL proteins, which constitute an important family of alternative splicing regulators. Sequestration of MBNL proteins results in the mis-splicing of its regulated transcripts. Previous work has demonstrated that pentamidine, a diamidine which is currently FDA-approved as an anti-parasitic agent, was able to partially reverse mis-splicing in multiple DM1 models, albeit at toxic concentrations. In this study, we characterized a series of pentamidine analogues in order to determine their ability to reverse mis-splicing and their toxicity *in vivo*. Experiments in cell and mouse models demonstrated that compound **13**, also known as furamidine, effectively reversed mis-splicing with equal efficacy and reduced toxicity compared to pentamidine.

## Graphical Abstract

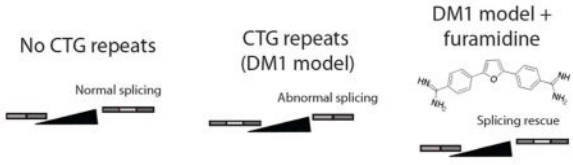


## INTRODUCTION

Myotonic dystrophy type 1 (DM1) is an inherited disorder characterized by myotonia, muscle wasting, insulin resistance, cardiomyopathy, and cognitive dysfunctions[1,2,3]. As a

*Corresponding Author: To whom correspondence should be addressed. aberglun@uoregon.edu.

**Conflicts of Interest:** The authors declare the following competing financial interest(s): The University of Oregon and J. Andrew Berglund have patented pentamidine and analogues (US 8,436,049 B2) as possible compounds for therapeutic use in Myotonic Dystrophy.

Supporting Information Available: Synthetic methods and spectroscopic characterization of compounds used in this study are provided herein. This material is available free of charge via the Internet at http://pubs.acs.org.

trinucleotide repeat disorder, individuals with DM1 possess aberrant expansions of DNA repeats. In particular, DM1 is caused by an expansion of CTG repeats in the 3′ untranslated region of the DM protein kinase (*DMPK*) gene. These expansions can contain between 50 and thousands of repeats [4,5,6]. When transcribed into RNA, CUG expansions serve as binding sites for RNA-binding proteins, thereby aggregating and sequestering these proteins from their canonical functions [7,8]. One such class of proteins is the muscleblind-like (MBNL) family of splicing factors. Consistent with this model, *in vivo* fluorescent hybridization experiments of expanded CUG repeats demonstrated that they form nuclear aggregates, or foci, with MBNL proteins[9]. Members of the MBNL family, including MBNL1, MBNL2, and MBNL3, regulate the alternative splicing of over 90 tissue-specific transcripts, and are also involved in RNA localization and processing events[10,11]. DM1 phenotypes are the result of mis-spliced, MBNL-regulated events. In support of this, two of the transcripts mis-spliced in DM1, pertaining to the insulin receptor (*INSR*) and chloride channel (*CLCN1*) genes, have been directly correlated with two key symptoms experienced by DM1 patients: insulin insensitivity and myotonia, respectively[12,13,14]. While there are no current treatments for this disease, approaches under development aim to reduce MBNL sequestration by CUG repeats and thereby reverse mis-splicing and associated symptoms [15,16,17,18,19]. One strategy to achieve this is through the administration of small molecules that can bind nucleic acids and ultimately prevent formation of CUG: MBNL aggregates [20,21].

Recent work from our lab has found that the small molecule pentamidine and the related molecule heptamidine were able to rescue mis-spliced events and reduce CUG RNA levels in both cell and mouse models of DM1 [15,22]. Pentamidine, a diamidine composed of two phenyl amidine groups joined by a five-carbon methylene linker (Figure 1), is currently FDA-approved for the treatment of various parasitic infections, including pneumocystic pneumonia, leishmaniasis, and trypanosomiasis[23]. While pentamidine's biomolecular target within parasitic organisms remains unclear, previous work has demonstrated that it is capable of binding the minor groove of AT-rich DNA with high affinity [24]. This is supported by the fact that pentamidine has a number of important structural features which promote DNA interaction: the amidines provide minor groove recognition by forming hydrogen bonds with base pair acceptors, the overall positive charge of the molecule helps to offset the negatively charged DNA backbone, and the flat arenes connected by a conformationally flexible linker promote incorporation into, and stacking within, the walls of the narrow minor groove of AT-rich DNA [25,26]. However, given our previous observation that pentamidine also modestly interacts with CTG DNA *in vitro* and reduces CUG RNA levels *in vivo* [22], it is possible that AT-rich DNA is not the only (or even the primary) target of diamidines within the DM1 framework. Our observations are consistent with a model in which pentamidine inhibits transcription of CTG DNA although other possible mechanisms (including the promoting of CUG RNA degradation) remain to be explored.

While extensive SAR and analogue studies have been performed in order to optimize the structural features of diamidines against eukaryotic parasites [25, 27–29], there is sparse information concerning which physiochemical properties of pentamidine are necessary to rescue mis-splicing in a DM1 model. An exploration of pentamidine derivatives varying in methylene linker length (3–9 carbons) demonstrated that increasing linker length correlated

with increasing efficacy in a cell model, but also resulted in decreased solubility and increased toxicity; ultimately, seven–carbon derivative, heptamidine, demonstrated the highest efficacy while remaining water soluble [22]. However, heptamidine also demonstrated high toxicity in a mouse model, as some mice were unable to tolerate a standard, one-week daily regimen. Modifications to other regions of pentamidine or heptamidine (i.e., the phenyl amidine groups) have not been previously explored in DM1 models. In this study, we present the results of an SAR study based on pentamidine and heptamidine. Analogues were synthesized containing various substitutions that alter the size, degrees of freedom, hydrophobicity and number of hydrogen bond donors of the parent compounds. The analogues' ability to ameliorate splicing defects in cellular and transgenic mouse models of DM1, as well as their toxicity relative to the parent compound, were assessed.

## RESULTS AND DISCUSSION

### SAR study identifies key structural elements of pentamidine required for splicing rescue

Diamidines such as pentamidine share three key structural features that are critical for their anti-parasitic activity: a semi-curved shape (or the ability to adopt this shape), two positively charged terminal amidine groups with hydrogen bonding ability, and a relatively flat conformation with some flexibility in the methylene linker [26]. We hypothesized that the structural requirements for therapeutic activity as an anti-parasitic may be similarly important for mis-splicing rescue in a DM1 cell model, given our model that pentamidine may function through transcription inhibition of CTG repeat DNA and thus may largely be dependent on its DNA-binding properties in order to reverse mis-splicing. To this end, we created a series of structures (**2a–c**, Figure 2a) that were derived from pentamidine but lacked the second amidine group (**2a**), both the second amidine group and the second ether linkage (**2b**), or an entire phenoxy-amidine group (**2c**). The compounds were also distinct from pentamidine in that they had shorter methylene linkers: compound **2a** possessed a three-carbon methylene linker, **2b** a four-carbon methylene linker, and **2c** an un-substituted butyl chain.

The HeLa cell DM1 splicing assay is a commonly employed system used to assess the efficacy of potential treatments for this disease *in vivo*. While HeLa cells do not endogenously possess CTG expansions in their genome, overexpression of 960 interrupted CUG repeats ($CUG_{960}$) *in vivo* recapitulates DM1 molecular phenotypes [7,22,30]. When these cells are co-transfected with MBNL-regulated minigenes, the resulting splicing variations can be analyzed in the presence or absence of potential compounds. One well-characterized minigene, *INSR*, corresponds to exons 10–12 (and the intervening introns) of the human insulin receptor gene (Figure 2b). The *INSR* minigene demonstrates splicing defects upon co-transfection with $CUG_{960}$[15]. Within the *INSR* minigene, MBNL promotes the inclusion of alternatively spliced exon 11. Exon 11 is included in 76 ± 6% of *INSR* minigene transcripts when CUG repeats were absent. Upon co-transfection of $CUG_{960}$, this value decreased to 49 ± 3%. All compounds were initially screened with this assay to determine if they could induce reversal of exon 11 inclusion levels back to those exhibited in cells lacking the transfected CUG repeats.

Interestingly, our splicing results demonstrated removal of one amidine group (**2a**) did not ablate the ability to rescue *INSR* splicing (Figures 2c and 2d), as compound **2a** demonstrated dose-dependent rescue of mis-splicing through 60 μM in the HeLa cell system. The calculated concentration necessary to observe 50% splicing rescue ($EC_{50}$) for this compound was 47 ± 5 μM, which is greater than the value calculated for pentamidine (31 ± 2 μM). However, when compared to the $EC_{50}$ value of propamidine[22] (42 ± 19 μM), which similarly possesses a four-carbon linker, there is no significant difference. We were unable to observe full splicing rescue with **2a** before extensive cell death occurred. In contrast, removal of the second phenolic linkage in conjunction with the amidine group (**2b**) resulted in strongly reduced ability to rescue mis-splicing, as little rescue was observed by 20 μM (Figures 2c and 2d). Due to the toxicity observed with compound **2b** before any substantial rescue was observed, we were unable to calculate a proper $EC_{50}$ value, and therefore no definitive conclusions can be made about the importance of the ether linkage for splicing rescue. Finally, compound **2c**, which consisted only of a single phenyl amidine group with a butoxy chain, demonstrated significantly reduced potential for mis-splicing rescue with an $EC_{50}$ value of 237 ± 33 μM (Figures 2c and 2d). Taken together, these results suggest that the presence of only one phenoxyamidine is sufficient in pentamidine derivatives to induce a partial rescue of the *INSR* splicing event, as long as the other phenoxy group is maintained. This is surprising considering amidines provide H-bond donating –NH groups that interact with H-bond acceptors (such as those present in the minor groove of AT-rich sequences), and therefore both groups are presumed to play a crucial role in the hydrogen bonds that stabilize pentamidine's interaction with AT-rich DNA [25].

## Heptamidine derivatives vary in splicing rescue efficacy

Heptamidine, a derivative of pentamidine with a seven carbon methylene linker, rescued *INSR* mis-splicing with an $EC_{50}$ value of 9 ± 1 μM in the HeLa cell system while still retaining its water solubility [22]. It was similarly able to rescue or partially rescue two endogenous splicing events in a transgenic DM1 mouse model. Nonetheless, heptamidine was observed to be fairly toxic in both the cell and mouse models. Because of these previously reported results, we opted to synthesize two heptamidine derivatives (**4** and **6**, Figure 3a) to determine if we could increase or maintain efficacy and decrease toxicity. In compound **4**, we placed the amidine groups in the meta-position relative to the phenoxy linkage, rather than in the para-position. In compound **6**, a methoxy group was added in the ortho-position relative to the phenoxy linkage. The five carbon version of both of these compounds were previously synthesized and tested in a rat model for *P.carinii* pneumonia, where they varied in their toxicity in comparison to pentamidine [31].

In the DM1 HeLa cell model, compound **4** was able to produce almost complete dose-dependent mis-splicing rescue at 25 μM, but was also very toxic over the range tested (10 – 25 μM, Figures 3b and 3c). The $EC_{50}$ for this compound was 18 ± 7 μM, suggesting that compounds with amidine groups in a meta-position have half the efficacy of heptamidine. Compound **6** demonstrated significantly reduced potential for mis-splicing rescue with an $EC_{50}$ value of 97 ± 17 μM, more than tenfold the original $EC_{50}$ value calculated for heptamidine (Figures 3b and 3c). Furthermore, compound **6** demonstrated significant toxicity by 100 μM, and therefore full rescue was not achieved with this compound. As we

were unable to significantly reduce toxicity within the range of rescue for either heptamethylene-linked compound, we chose to focus on creating more effective five carbon linker compounds that were less toxic.

### *N*-substituted amidines do not reduce toxicity/increase efficacy *in vivo*

We next examined the previously reported strategy of substituting the amidine groups of the diamidine compounds, thereby producing *N*-substituted amidines [32, 33, 34]. The aim of creating *N*-substituted compounds was to increase the size of the molecule in order to reduce the concentration required to achieve full splicing rescue. Furthermore, we chose substitutions that increased hydrogen bonding ability or enhanced hydrophobic interactions, some of which have been previously examined in the context of anti-parasitic activity [35, 36]. We first synthesized a precursor molecule, which contained an un-substituted propyl chain (**8**, Figure 4a), to determine if the addition of a carbon chain somewhere other than within the central methylene domain would increase the efficacy of splicing rescue. Compound **8** was able to reach full splicing rescue by 150 μM, and was not toxic over the range of rescue (Figure 4b). While the $EC_{50}$ value of the compound was 70 ± 12 μM, the lack of toxicity exhibited with this compound was a promising result that prompted us to examine whether substituting the propyl chain would increase efficacy and maintain low toxicity. We created two series of compounds with either a phenylpropyl or *N,N*-dimethylaminopropyl substituent, with each series consisting of 3-carbon, 5-carbon, and 7-carbon variants for both substitution types (**9a**–**9c** and **10a**–**10c**, Figure 4c).

The phenyl-substituted series (**9a**–**9c**) demonstrated increased efficacy compared to pentamidine and similar efficacy compared to heptamidine, with compounds **9b** and **9c** producing $EC_{50}$ values of 10.5 ± 5.4 and 10.4 ± 2.9 μM, respectively. However, all compounds in this series were too toxic within our cell assay to observe full rescue (Figure 4d). Conversely, the *N,N*-dimethylamino series (**10a**–**10c**) demonstrated decreased efficacy, with compounds **10a** through **10c** demonstrating $EC_{50}$ values in the 200–300 μM range; all compounds were also observed to be too toxic to reach full rescue, although they were considerably less toxic then their phenyl-substituted counterparts (Figure 4e). As previously observed, both series demonstrated a trend towards increased efficacy with increasing length of the central linker region.

While the observed toxicity of these compounds was qualitatively informative, we wanted to quantitate toxicities and compare compounds based on these values alone. To quantify relative toxicities, we devised a flow cytometry-based cell viability assay using propidium iodide, a membrane-impermeant dye which binds exposed DNA in dead cells. Both phenylpropyl and *N,N*-dimethylaminopropyl series, as well as pentamidine and heptamidine, were tested in the DM1 cell model using the same cell culture conditions as for the splicing assays. The cytotoxicity of each compound was assessed by calculating the concentration necessary to observe 50% cell death, or $IC_{50}$ value (Table 1). Higher $IC_{50}$ values indicate lower toxicity. These results were then used to calculate $EC_{50}$:$IC_{50}$ ratios, which provided us with the criteria for identifying compounds that are both effective and less toxic than pentamidine. For example, the $EC_{50}$:$IC_{50}$ of pentamidine was calculated as 0.48 (value attained by dividing 31 μM /64 μM), which demonstrates that twice as much pentamidine is

necessary to see 50% cell death as is needed to see 50% *INSR* splicing rescue. A value above 0.48 indicates that the compound had a smaller window to rescue splicing before causing cell death. Therefore, desirable compounds would have an $EC_{50}$:$IC_{50}$ value lower than 0.48. However, smaller $EC_{50}$:$IC_{50}$ ratios could also result from structures that were less effective in splicing rescue compared to pentamidine but were less toxic (for example, an $EC_{50}$ of 200 μM and $IC_{50}$ of 500 μM would yield a ratio of 0.4), and so both $EC_{50}$ and $IC_{50}$ values were considered individually as well.

Since we were only interested in derivatives with higher or equal efficacy to pentamidine, a more efficient alternative to pentamidine has to meet two criteria: a lower $EC_{50}$ value than pentamidine's calculated value of 31 μM as well as an $EC_{50}$:$IC_{50}$ value lower than 0.48. All compounds except **8** had $EC_{50}$:$IC_{50}$ values above 0.48 due to their low $IC_{50}$ values. While structure **8**, demonstrated a promising $EC_{50}$:$IC_{50}$ values of 0.20, it was half as effective as pentamidine in the splicing assay ($EC_{50}$ value of 70 ± 12 μM). Since none of the phenyl or substituted compounds (**9a–9c**, **10a–10c**) met these criteria, we concluded these substitutions are not more effective than pentamidine at improving splicing defects *in vivo*.

## Compounds 12 and 13 effectively rescue mis-splicing of two minigenes

The final set of compounds analyzed consisted of three conformationally restricted molecules, planar compounds **11**–**13** (Figure 5a). Both linearity and planarity have been previously implicated in promoting binding of these molecules to the minor groove of DNA [37, 38]. Minor groove binding is best mediated when the curvature of the inner atoms of a molecule are around 20 Å, but recent studies demonstrated that linear compounds can also bind the minor groove of DNA through water-mediated interactions [25,39]. Compounds **11** and **12** are essentially linear, while **13** has a concave shape, considered best suited for binding in the minor groove of DNA [37].Planarity, meanwhile, is commonly associated with intercalation; however, CD spectra of **12** and **13** demonstrate that neither compound intercalates with DNA[39]. Furthermore, compound **11**, a 2,7-bisamidine carbazole, has been previously demonstrated to bind both GC and AT DNA [40,41]. Despite this fact, **11** was the least effective in the DM1 splicing assay ($EC_{50}$ value of 125 μM) and was also the most toxic with an $IC_{50}$ value of 134 ± 56 μM (Figure 5b). In contrast, both **12** and **13** demonstrated similar $EC_{50}$ values to pentamidine (31 ± 4 and 30 ± 4 μM, respectively). Compound **12** was also significantly less toxic than **11** with an $IC_{50}$ value of 210 ± 19.3 μM, making it the molecule with the lowest $EC_{50}$:$IC_{50}$ ratio. Interestingly, at the highest concentration tested (150 μM, not shown), **12** increased exon 11 inclusion levels above that of wild type. While a reproducible $IC_{50}$ value could not be attained for compound **13** because the fluorescence of the furan group produced high background in our flow cytometry assay, this molecule was also observed to be non-toxic over the range of rescue. High levels of cell death were not observed with this compound in the 20–80 μM range, unlike pentamidine. Based on these results, it was clear that both **12** and **13** were the most effective compounds and have a larger window of activity compared to pentamidine and heptamidine.

DM1 pathophysiology is the result of numerous mis-splicing events across skeletal muscle, striated muscle, and neuronal tissues [2, 42]. Therefore, small molecule approaches which aim

to reduce DM1 pathology must target multiple MBNL1-dependent mis-splicing events to be successful. In light of this fact, we tested compounds **12** and **13** for their ability to rescue splicing of another transiently transfected minigene, cardiac troponin T (*TNNT2*). MBNL proteins are negative regulators of exon 5 in *TNNT2*, thereby facilitating the exclusion of this exon in the final mRNA product (Figure 5c). Typical inclusion levels of *TNNT2* exon 5 within the HeLa cell system were observed at 69 ± 4%, and this value increased to 87 ± 3% in the presence of $CUG_{960}$ (Figure 5d). Compound **12** was able to achieve full mis-splicing reversal by 120 μM, while **13** achieved full mis-splicing reversal by 80 μM. The calculated $EC_{50}$ values for *TNNT2* rescue by **12** and **13** were 77 ± 6 and 42 ± 7 μM, respectively. The difference observed in $EC_{50}$ values between *INSR* and *TNNT2* systems has been previously observed with other diamidine derivatives [22] and may be due to the fact that MBNL targets differ in the amount of MBNL they require in order to be properly regulated [43]. These results suggest that planarity, but not linearity, of diamidine compounds may be an important component for splicing rescue.

While reversal of mis-splicing is an important measure of the efficacy of small molecules within the DM1 framework, it is also important to determine if these molecules alter splicing in the absence of CUG repeats. We therefore performed control splicing experiments with both compounds **12** and **13** in the absence of transfected $CUG_{960}$ (Figure S1). With the *INSR* minigene, inclusion levels of exon 11 vary between ~70% and ~80 %. This range of exon 11 inclusion is likely due to a combination of experimental nuances, including variability in cell passage number, cell plating, and transfection efficiency. Compound **12** increased inclusion of exon 11 to 90 ± 2 % with a 60 μM dosage (Figure S1a). In contrast, compound **13** treatment didn't modulate exon 11 inclusion splicing above or below the expected range, even at an 80 μM dosage (81± 4% exon inclusion observed, Figure S1b). Similar trends were observed for the control experiment with *TNNT2* minigene splicing. Compound **12** again demonstrated a dose-dependent reduction of exon 5 inclusion in the absence of CUG repeats, while compound **13** did not alter *TNNT2* splicing over the tested range (Figure S1c–d). These results indicate compound **12** modulates splicing through mechanisms beyond targeting the CUG repeats. Due to the non-specific results with compound **12,** we focused the remainder of our studies on compound **13**.

## Compound 13 reduces nuclear foci *in vivo*

A distinguishing characteristic of DM1 cells is that CUG RNA aggregate with MBNL proteins to form nuclear foci [9]. To directly visualize the effect of compound **13** on MBNL sequestration, CUG foci formation and nuclear MBNL1 localization were examined in the HeLa cell system in the presence or absence of these compounds. Anti-MBNL1 antibody MB1a (4A8, MDA Monoclonal Antibody Resource) was used to probe for MBNL1 localization, and a CAG probe was employed to bind CUG RNA [44]. Untreated HeLa cells not transfected with $CUG_{960}$ demonstrated diffuse localization of MBNL1 throughout the nucleus (Figure 6, row 1). Upon transfection of the $CUG_{960}$ plasmid, characteristic RNA foci were observed (Figure 6, row 2). Complete co-localization of MBNL1 was not observed, most likely a result of varying CAG-probe accessibility to CUG RNA once in aggregate form.

Upon addition of 80 μM of compound **13**, we observed a decrease in the number of foci per cell when compared to the transfected controls (Figure 6, rows 4 & 5). This result is comparable to that observed for 50 μM pentamidine (Figure 6, row 3). While most cells treated with **13** still possessed modest numbers of nuclear foci, there was an 89% reduction with compound treatment ($n = 121$, $p < 0.05$), which was statistically significant. Nuclear MBNL levels in treated cells were observed to be more diffuse and evenly spread compared to untreated cells, despite the persistence of some foci. These results indicate that compound **13** is able to disrupt formation of the CUG: MBNL complex.

### Compound 13 rescues mis-splicing in a DM1 mouse model

The $HSA^{LR}$ mouse model expresses 220 CUG repeats under the skeletal promoter [47]. In this model, two well-characterized endogenous pre-mRNAs were analyzed: *Clcn1*, which has been linked to myotonia when mis-splicing occurs, and *Atp2a1* (also known as *Serca*), which encodes a sarcoplasmic calcium ATPase and exhibits a broad splicing differential in DM1[14, 48]. In *Clcn1*, MBNL is responsible for promoting the exclusion of exon 7a. Wild type adult mice demonstrated 7a included at 5 ± 0.9 %, this value increased 8-fold to 39 ± 2 % in $HSA^{LR}$ mice (Figure 7a). Treatment with a 10 and 20 mg/kg regimen of compound **13** resulted in a dose-dependent reversal of exon 7a levels to 11 + 3 %, which was close to a full rescue.

Similar rescue of splicing was observed for the *Atp2a1* event, for which MBNL is a positive regulator of exon 22 (Figure 7b). Wild type adult mice included exon 22 at 100 ± 0.2 %, while $HSA^{LR}$ mice only included this exon at 28 ± 2 %. Treatment with 10 and 20 mg/kg of compound **13** over 7 days caused exon 22 inclusion levels to shift to 64 ± 4 % and 83 ± 4 %, respectively. While a full rescue was not observed for either splicing event, the rescue of mis-splicing was significant at both dosages and for both events investigated. These data demonstrate that compound **13** was able to reverse mis-splicing in DM1 mice with similar activity compared to heptamidine and did so without the observed toxicity.

## CONCLUSIONS

An appropriate assessment of small molecules as potential lead compounds for development of therapeutics for DM1 requires two key considerations: the effectiveness of the compound in biological systems as well as the toxicity of the compound. Previous work demonstrated the efficacy of pentamidine and various pentamidine derivatives as potential lead compounds for DM1 models [15,22], but cytotoxicity and lethality in transgenic mice had not been thoroughly explored as secondary criteria for success. Here, we report an SAR study of pentamidine and heptamidine derivatives in the context of DM1 molecular pathology. A deconstructionist approach was used to determine the structural elements most critical for splicing rescue of the *INSR* minigene in a DM1 HeLa cell model. Results from these studies demonstrated that one amidine group was sufficient for splicing rescue; however, both phenoxy groups were necessary to retain efficacy in the DM1 cell model.

After thorough examination of previous work on diamidines, we synthesized three series of molecules varying in amidine substitution and central linker length, as well as planarity. We uncovered two planar systems, compounds **12** and **13**, which exhibited similar activity to

pentamidine but are both considerably less toxic *in cellulo* and one was less toxic in DM1 transgenic mice. Control splicing experiments did demonstrate that compound **12** (but not compound **13**) caused splicing changes in the absence of CUG repeats, suggesting that the splicing rescue observed in the DM1 HeLa cell model may be a result of global effects on splicing. In future studies, it would be interesting to examine the effects of compounds **12** and **13** on all endogenous splicing events through RNA-seq analyses of treated DM1 model cells and/or transgenic DM1 mice. For the purposes of this study, however, the results from these control experiments prompted us to focus on compound **13**, the best compound from our screen with demonstrated specificity for CUG repeat molecular pathology.

Fluorescent microscopy further confirmed that **13** reduced pathological nuclear aggregates. The reduction of nuclear aggregates is consistent with several different mechanisms. Pentamidine has been previously demonstrated to reduce CUG RNA levels, suggesting that it may inhibit transcription of CTG DNA or reduce the stability of the transcript [22]. Another possibility is that these molecules are able to bind directly to CUG RNA and therefore displace MBNL proteins from nuclear aggregates, which is a commonly employed mechanism by many other compounds in the study of DM1 [20, 21, 44]. Future studies will aim to distinguish if amidines work through one or both of these mechanisms or through additional mechanisms.

## EXPERIMENTAL METHODS

General Methods for Synthesis. $^{1}H$ and $^{13}C$ NMR spectra were obtained on a Varian Mercury 300 MHz spectrometer ($^{1}H$: 300.09) or Inova 500 MHz spectrometer ($^{1}H$: 500.10 MHz, $^{13}C$: 125.75 MHz). Chemical shifts (δ) are expressed in ppm downfield from tetramethylsilane (TMS) using non-deuterated solvent present in the bulk deuterated solvent ($CDCl_3$: $^{1}H$ 7.26 ppm, $^{13}C$ 77.16 ppm; DMSO-$d_6$: $^{1}H$ 2.50 ppm, $^{13}C$ 39.52 ppm). All NMR spectra were processed using MestReNova NMR processing software. High resolution mass spectra were acquired using a JEOL MS-Route mass spectrometer. THF was distilled from sodium prior to use. The purity of all compounds was >95% and was confirmed by HPLC analysis using an Agilent 1100 Series chromatograph with Diode Array Detector (DAD) UV detection. The chromatographic method utilized a Waters XTerra MS C-18 3.9 × 100 mm, 3.5 μm column; UV detection wavelength = 240 nm; flow rate = 1 mL/min; gradient = 0–100% (0.1% TFA in acetonitrile) over 25 min with a hold of 5 min at 100% (0.1% TFA in acetonitrile); the aqueous mobile phase contained 0.1% TFA. All chemicals were of reagent grade and used as obtained from manufacturers. For compound synthesis and characterization, see Supporting Information text.

Splicing Analysis in Cell Culture. Approximately $2.1 \times 10^5$ cells were plated in 6-well plates and 1 μg total plasmid (either all pcDNA3 for mock treatment or 500 ng pcDNA3 and 500 ng $CUG_{960}$ plasmid) was transfected 24–36 h later using Lipofectamine 2000 (Invitrogen). After transfection, cells were incubated in OPTI-mem (GIBCO) for 6 h and then washed with 1x PBS and placed in DMEM with GLUTAMAX (GIBCO) supplemented with 10% FBS (v/v) (GIBCO) along with indicated concentrations of compounds. Cells were harvested 18 h after addition of compound and RNA was isolated immediately using an RNeasy kit (QIAGEN) and frozen at −80°C until use. RNA concentration was determined

using a NanoDrop (Thermo). After DNase treatment, RNA was reverse transcribed with SuperScript II and a plasmid specific reverse primer. This cDNA was then subjected to PCR (22 rounds for *INSR* or 24 rounds for *TNNT2*). Resulting PCR products were then run on a 6% (w/v) 19:1 native polyacrylamide gel containing 0.5x TB at 300 V for 90 min. The gel was then stained with 1x SYBR I dye (Applied Biosystems) in 0.5xTB for 15 min. Quantification of bands was performed using the Alpha Imager HP software from Alpha Innotech. $EC_{50}$ values were determined by performing linear regression analysis of the data using Excel (Microsoft), and determining the concentration which would result in 50% splicing rescue, calculated as halfway between wild type and disease state levels of exon inclusion. Statistical significance of splicing change due to molecule treatment was calculated by t-test in excel. T-tests compared splicing values of treatment to splicing values in the disease control. Each data set was analyzed for equal/unequal variance using F-test in excel in order to determine appropriate T-test.

The following primers were used. For the *TNNT2* minigene, the RT primer was 5′ AGC ATT TAG GTG ACA CTA TAG AAT AGG G. The forward primer for PCR was 5′ GTT CAC AAC CAT CTA AAG CAA GAT G and the reverse primer was 5′ GTT GCA TGG CTG GTG CAG G. For the *INSR* minigene, the RT primer was 5′ GCT GCA ATA AAC AAG TTC TGC. The forward primer for PCR was 5′ CGA ATT CGA ATG CTG CTC CTG TCC AAA GAC AG, and the reverse primer was 5′ TCG TGG GCA CGC TGG TCG AG. The *TNNT2* minigene was a gift from the lab of Thomas Cooper and the *INSR* minigene was a gift from Nicholas Webster.

Cell Viability Analysis. Cells were plated and transfected as in the splicing analysis protocol. After an 18 h incubation with compound, both dead (floating) cells and live (adhered) cells were carefully harvested into 2 mL, light-sensitive tubes to avoid rupturing and lysis. Cells were centrifuged at 13,000 rcf for 3 minutes and residual media was aspirated from the tubes, leaving cell pellets. A 100 μL volume of 1x PBS was then added to the cell pellets and each was vortexed on high to re-suspend cells in buffer. Cell suspensions were then incubated at room temperature for 15 minutes with 1 μg/mL final concentration of propidium iodide. Cell suspensions were then analyzed using an Attune Acoustic Focusing Flowcytometer (Life technologies). $IC_{50}$ values were determined with KaleidaGraph (Synergy) software using the equation

$$Y = \frac{m_3}{1 + \left(\frac{m_0}{m_1}\right)^{m_2}}$$

where $m_0$ = small molecule concentration, $m_1 = IC_{50}$, $m_2$ = Hill coefficient, and $m_3$= fraction of MBNL1 bound without small molecule present. Errors were determined by calculating the standard deviation of triplicate data.

Fluorescent Microscopy. Imaging of foci was performed as previously described[15]. Briefly, HeLa cells were plated in 6-well plates onto coverslips and transfected with 500 ng of $CUG_{960}$ plasmid for each experiment. After transfection, respective compounds (pentamidine, 12, or 13) were added in the indicated concentrations and the cells were fixed

16 h later. Cells were fixed with 4% PFA and washed in 1× PBS, then permeabilized with 0.5% triton X-100, in 1× PBS. Cells were prewashed with 30% formamide, 2× SSC. Cells were then probed overnight at 37 °C with a Cy3 $CAG_{10}$ probe (IDT, IA). The next day cells were washed 30% formamide, 2× SSC, and then with 1× SSC. Cells were next washed twice in 1× PBS and then probed overnight with the MB1a anti-MBNL1 antibody (1:5000 dilution, MDA Monoclonal Antibody Resource) in 1× PBS. Cells were washed with 1× PBS and incubated with donkey anti-mouse Alexa 488 (1:500 dilution). Cells were washed 2 times with 1× PBS and then mounted onto glass slides using hard-set mounting media that contains DAPI (Vectashield). Cells were imaged on an Olympus Fluoview FV1000 with a Bx61 scope. Nuclear foci for each cell were quantified using ImageJ. F test analyses were performed to determine if the data sets possessed equal or unequal variances. Appropriate T-test analyses were then performed using Excel (Microsoft).

Compound 13 treatments of mice. Homozygous gender-matched, *HSA*LR transgenic mice of 10–14 wks age were treated with compound 13 (dissolved in 5% glucose solution) at the indicated dose by daily intraperitoneal injection for 7 d. Control mice received 5% glucose injections. Mice were sacrificed 1 d after the final injection and quadriceps muscle was obtained for splicing analysis. RNA was isolated, reverse transcribed, and amplified by PCR, and analyzed on agarose gels using a fluorimager.

## Supplementary Material

Refer to Web version on PubMed Central for supplementary material.

## Acknowledgments

This work was supported by grant AR0599833 from NIAMS/NIH and Myotonic Dystrophy Foundation (fellowship to Micah Bodner). We thank T. Cooper for the gifts of *TNNT2* and $DMPK_{960}$ minigenes and N. Webster for the *INSR* minigenes. HRMS were obtained at the Biomolecular Mass Spectrometry Core of the Environmental Health Sciences Core Center, Oregon State University, supported by grant #P30-ES00210, National Institute of Environmental Health Sciences, National Institutes of Health. We also thank the MDA Monoclonal Resource for providing the MBNL1 antibody.

## Abbreviations used

| | |
|---|---|
| **DM1** | Myotonic dystrophy type 1 |
| **DMPK** | DM protein kinase gene (human) |
| **MBNL1** | Muscleblind-like 1 |
| **INSR** | Insulin receptor gene (human) |
| **TNNT2** | Cardiac troponin T gene (human) |
| **CLCN1** | Chloride channel (human) |
| **$CUG_{960}$** | Plasmid containing 960 CUG repeats |
| **Clcn1** | Chloride channel (mouse) |
| **Atp2a1** | Sarcosplasmic ATPase Atp2a1 (mouse) |

| | |
|---|---|
| **$EC_{50}$** | Half maximal concentration (splicing rescue) |
| **$IC_{50}$** | Half maximal concentration (cell toxicity) |

## References


1. Harper, PS. Major problems in neurology: myotonic dystrophy;. WB Saunders; London: 2001.
2. Ranum LP, Cooper TA. RNA-mediated neuromuscular disorders. Annu Rev Neurosci. 2006; 29:259–277. [PubMed: 16776586]
3. Cho DH, Tapscott SJ. Myotonic dystrophy: emerging mechanisms for DM1 and DM2. Biochim Biophys Acta, Mol Basis Dis. 2007; 1772:195–204.
4. Harley HG, Brook JD, Rundle SA, Crow S, Reardon W, Buckler AJ, Harper PS, Housman DE, Shaw DJ. Expansion of an unstable DNA region and phenotypic variation in myotonic dystrophy. Nature. 1992; 355(6360):545–546. [PubMed: 1346923]
5. Mahadevan M, Tsilfidis C, Sabourin L, Shutler G, Amemiya C, Jansen G, Neville C, Narang M, Marcelo J, O'Hoy K, Leblond S, Earle-Macdonald J, de Jong PJ, Wieringa B, Korneluk RG. Myotonic dystrophy mutation: an unstable CTG repeat in the 3′ untranslated region of the gene. Science. 1992; 255:1253–1255. [PubMed: 1546325]
6. O'Rourke JR, Swanson MS. Mechanisms of RNA-mediated disease. J Biol Chem. 2009; 284:7419–7423. [PubMed: 18957432]
7. Ho TH, Savkur RS, Poulos MG, Mancini MA, Swanson MS, Cooper TA. Colocalization of muscleblind with RNA foci is separable from mis-regulation of alternative splicing in myotonic dystrophy. J Cell Sci. 2005; 118(13):2923–2933. [PubMed: 15961406]
8. Osborne RJ, Thornton CA. RNA dominant diseases. Hum Mol Genet. 2006; 15:162–69.
9. Fardaei M, Rogers MT, Thorpe HM, Larkin K, Hamshere MG, Harper PS, Brook JD. Three proteins, MBNL, MBLL and MBXL, co-localize *in vivo* with nuclear foci of expanded-repeat transcripts in DM1 and DM2 cells. Hum Mol Genet. 2002; 11:805–814. [PubMed: 11929853]
10. Wang ET, Cody NA, Jog S, Biancolella M, Wang TT, Treacy DJ, Luo S, Schroth GP, Housman DE, Reddy S, Lécuyer E, Burge CB. Transcriptome-wide regulation of pre-mRNA splicing and mRNA localization by muscleblind proteins. Cell. 2012; 15:710–724. [PubMed: 22901804]
11. Konieczny P, Stepniak-Konieczna E, Sobczak K. MBNL proteins and their target RNAs, interaction and splicing regulation. Nucleic Acids Res. 2015; 42(17):10873–87. [PubMed: 25183524]
12. Kanadia RN, Johnstone KA, Mankodi A, Lungu C, Thornton CA, Esson D, Timmers AM, Hauswirth WW, Swanson MS. A muscleblind knockout model for myotonic dystrophy. Science. 2003; 302:1978–1980. [PubMed: 14671308]
13. Philips AV, Timchenko LT, Cooper TA. Disruption of splicing regulated by a CUG-binding protein in myotonic dystrophy. Science. 1998; 280:737–741. [PubMed: 9563950]
14. Mankodi A, Takahashi MP, Jiang H, Beck CL, Bowers WJ, Moxley RT, Cannon SC, Thornton CA. Expanded CUG repeats trigger aberrant splicing of ClC-1 chloride channel pre-mRNA and hyperexcitability of skeletal muscle in myotonic dystrophy. Mol Cell. 2002; 10:35–44. [PubMed: 12150905]
15. Warf MB, Nakamori M, Matthys CM, Thornton CA, Berglund JA. Pentamidine reverses the splicing defects associated with myotonic dystrophy. Proc Natl Acad Sci US A. 2009; 106:18551–18556.
16. Arambula JF, Ramisetty SR, Baranger AM, Zimmerman SC. A simple ligand that selectively targets CUG trinucleotide repeats and inhibits MBNL protein binding. Proc Natl Acad Sci US A. 2009; 106:16068–16073.
17. Nakamori M, Gourdon G, Thornton CA. Stabilization of expanded (CTG)•(CAG) repeats by antisense oligonucleotides. Mol Ther. 2011; 19:2222–2227. [PubMed: 21971425]
18. Lee JE, Bennett CF, Cooper TA. RNase H-mediated degradation of toxic RNA in myotonic dystrophy type 1. Proc Natl Acad Sci US A. 2012; 109:4221–4226.

19. Wheeler TM, Leger AJ, Pandey SK, MacLeod AR, Nakamori M, Cheng SH, Wentworth BM, Bennett CF, Thornton CA. Targeting nuclear RNA for *in vivo* correction of myotonic dystrophy. Nature. 2012; 488:111–115. [PubMed: 22859208]
20. Pushechnikov A, Lee MM, Childs-Disney JL, Sobczak K, French JM, Thornton CA, Disney MD. Rational design of ligands targeting triplet repeating transcripts that cause RNA dominant disease: application to myotonic muscular dystrophy type 1 and spinocerebellar ataxia type 3. J Am Chem Soc. 2009; 131:9767–9779. [PubMed: 19552411]
21. Childs-Disney JL, Hoskins J, Rzuczek SG, Thornton CA, Disney MD. Rationally designed small molecules targeting the RNA that causes myotonic dystrophy type 1 are potently bioactive. ACS Chem Biol. 2012; 7:856–862. [PubMed: 22332923]
22. Coonrod LA, Nakamori M, Wang W, Carrell S, Hilton CL, Bodner MJ, Siboni RB, Docter AG, Haley MM, Thornton CA, Berglund JA. Reducing levels of toxic RNA with small molecules. ACS Chem Biol. 2013; 8(11):2528–37. [PubMed: 24028068]
23. Bray PG, Barrett MP, Ward SA, De Koning HP. Pentamidine uptake and resistance in pathogenic protozoa: past, present and future. Trends Parasitol. 2003; 19(5):232–239. [PubMed: 12763430]
24. Edwards KJ, Jenkins TC, Neidle S. Crystal structure of a pentamidine-oligonucleotide complex: Implication for DNA-binding properties. Biochemistry. 1992; 31:7104–7109. [PubMed: 1643044]
25. Cory M, Tidwell RR, Fairly TA. Structure and DNA binding activity of analogues of 1,5-bis(4-amidinophenoxy)pentamidine (Pentamidine). J Med Chem. 1992; 35:431–438. [PubMed: 1738139]
26. Wilson WD, Tanious FA, Mathis AM, Tevis D, Hall JE, Boykin DW. Antiparisitic compounds that target DNA. Biochimie. 2008; 90:999–1014. [PubMed: 18343228]
27. Chaires JB, Ren J, Hamelberg D, Kumar A, Pandya V, Boykin DW, Wilson WD. Structural selectivity of aromatic diamidines. J Med Chem. 2004; 47:5729–5742. [PubMed: 15509172]
28. Bakunov SA, Svetlana M, Bakunova SM, Wenzler T, Barszcz T, Werbovetz KA, Brun R, Tidwell RR. Synthesis and antiprotozoal activity of cationic 2-phenylbenzofurans. J Med Chem. 2008; 51:6927–6944. [PubMed: 18841956]
29. Bakunova SM, Bakunov SA, Patrick DA, Kumar EVKS, Ohemeng KA, Bridges AS, Wenzler T, Barszcz T, Kilgore Jones S, Werbovetz KA, Brun R, Tidwell RR. Structure-activity study of pentamidine analogues as antiprotozoal agents. J Med Chem. 2009; 52:2016–2035. [PubMed: 19267462]
30. Warf MB, Berglund JA. MBNL binds similar RNA structures in the CUG repeats of myotonic dystrophy and its pre-mRNA substrate cardiac troponin T. RNA. 2007; 13:2238–2251. [PubMed: 17942744]
31. Tidwell RR, Jones SK, Geratz JD, Ohemeng KA, Cory M, Hall JE. Analogs of 1,5-di(4-amidinophenoxy)pentane (pentamidine) in the treatment of experimental *Pneumocystis carinii* pneumonia. J Med Chem. 1990; 33:1252–1257. [PubMed: 2319567]
32. Silva CF, Meuser MB, de Souza EM, Meirelles MN, Stephens CE, Som P, Boykin DW, Soeiro MN. Cellular effects of reversed amidines on *Trypanosoma cruzi*. Antimicrob Agents Chemother. 2007; 51(11):3803–3809. [PubMed: 17698624]
33. Munde M, Lee M, Neidle S, Arafa R, Boykin DW, Liu Y, Bailly C, Wilson WD. Induced fit conformational changes of a “reversed amidine” heterocycle: optimized interactions in a DNA minor groove complex. J Am Chem Soc. 2007; 129:5688–5698. [PubMed: 17425312]
34. Khalifa MK, Bodner MJ, Berglund JA, Haley MM. Synthesis of N-Substituted Aryl Amidines by Strong Base Activation of Amines. Tetrahedron Lett. 2015; 56:4109–4111. [PubMed: 26097266]
35. De Souza EM, Lansiaux A, Bailly C, Wilson WD, Hu Q, Boykin DW, Batista MM, Araújo-Jorge TC, Soeiro MN. Phenyl substitution of furamidine markedly potentiates its anti-parasitic activity against *Trypanosoma cruzi* and *Leishmania amazonensis*. Biochem Pharmacol. 2004; 68:593–600. [PubMed: 15276066]
36. Wong CH, Nguyen L, Peh J, Luu LM, Sanchez JS, Richardson SL, Tuccinardi T, Tsoi H, Chan WY, Chan HY, Baranger AM, Hergenrother PJ, Zimmerman SC. Targeting Toxic RNAs that cause myotonic dystrophy type 1 (DM1) with a Bisamidinium inhibitor. J Am Chem Soc. 2014; 136:6355–6361. [PubMed: 24702247]

37. Shaikh SA, Ahmed SR, Jayaram B. A molecular thermodynamic view of DNA-drug interactions: a case study of 25 minor-groove binders. Arch Biochem Biophys. 2004; 429:81–99. [PubMed: 15288812]

38. Miao Y, Lee MP, Parkinson GN, Batista-Parra A, Ismail MA, Neidle S, Boykin DW, Wilson WD. Out-of-shape DNA minor groove binders: induced fit interactions of heterocyclic dications with the DNA minor groove. Biochemistry. 2005; 44:14701–14708. [PubMed: 16274217]

39. Ismail A, Arafa RK, Brun R, Wenzler T, Miao Y, Wilson DW, Generaux C, Bridges A, Hall JE, Boykin DW. Synthesis, DNA affinity, and antiprotozoal activity of linear dications: terphenyl diamidines and analogues. J Med Chem. 2006; 49:5324–5332. [PubMed: 16913722]

40. Tanious FA, Wilson WD, Patrick DA, Tidwell RR, Colson P, Houssier C, Tardy C, Bailly C. Sequence-dependent binding of bis-amidine carbazole dications to DNA. Eur J Biochem. 2001; 268:3455–3464. [PubMed: 11422375]

41. Brendle JJ, Outlaw A, Kumar A, Boykin DW, Patrick DA, Tidwell RR, Werbovetz KA. Antileishmanial activities of several classes of aromatic dications Antimicrob. Agents Chemother. 2002; 46:797–807.

42. Charizanis K, Lee KY, Batra R, Goodwin M, Zhang C, Yuan Y, Shiue L, Cline M, Scottie MM, Xia G, Kumar A, Ashizawa T, Clark HB, Kimura T, Takahashi MP, Fujimura H, Jinnai K, Yoshikawa H, Gomes-Pereira M, Gourdon G, Sakai N, Nishino S, Foster TC, Ares M Jr, Darnell RB, Swanson MS. Muscleblind-like 2-mediated alternative splicing in the developing brain and dysregulation in myotonic dystrophy. Neuron. 2012; 75:437–450. [PubMed: 22884328]

43. Jog SP, Paul S, Dansithong W, Tring S, Comai L, Reddy S. RNA splicing is responsive to MBNL1 dose. PLoS ONE. 2012; 7(11):e48825. [PubMed: 23166594]

44. Holt I, Mittal S, Furling D, Butler-Browne GS, Brook JD, Morris GE. Defective mRNA in myotonic dystrophy accumulates at the periphery of nuclear splicing speckles. Genes to Cells. 2007; 12:1035–1048. [PubMed: 17825047]

45. Jahromi AH, Nguyen L, Fu Y, Miller KA, Baranger AM, Zimmerman SC. A novel CUGexp · MBNL1 inhibitor with therapeutic potential for myotonic dystrophy type 1. ACS Chem Biol. 2013; 8:1037–1043. [PubMed: 23480597]

46. Holt I, Mittal S, Furling D, Butler-Browne GS, Brook JD, Morris GE. Defective mRNA in myotonic dystrophy accumulates at the periphery of nuclear splicing speckles. Genes to Cells. 2007; 12:1035–1048. [PubMed: 17825047]

47. Mankodi A, Logigian E, Callahan L, McClain C, White R, Henderson D, Krym M, Thornton CA. Myotonic dystrophy in transgenic mice expressing an expanded CUG repeat. Science. 2000; 289(5485):1769–1773. [PubMed: 10976074]

48. Kimura T, Nakamori M, Lueck JD, Pouliquin P, Aoike F, Fujimura H, Dirksen RT, Takahashi MP, Dulhunty AF, Sakoda S. Altered mRNA splicing of the skeletal muscle ryanodine receptor and sarcoplasmic/endoplasmic reticulum Ca2+-ATPase in myotonic dystrophy type 1. Hum Mol Genet. 2005; 14:2189–2200. [PubMed: 15972723]

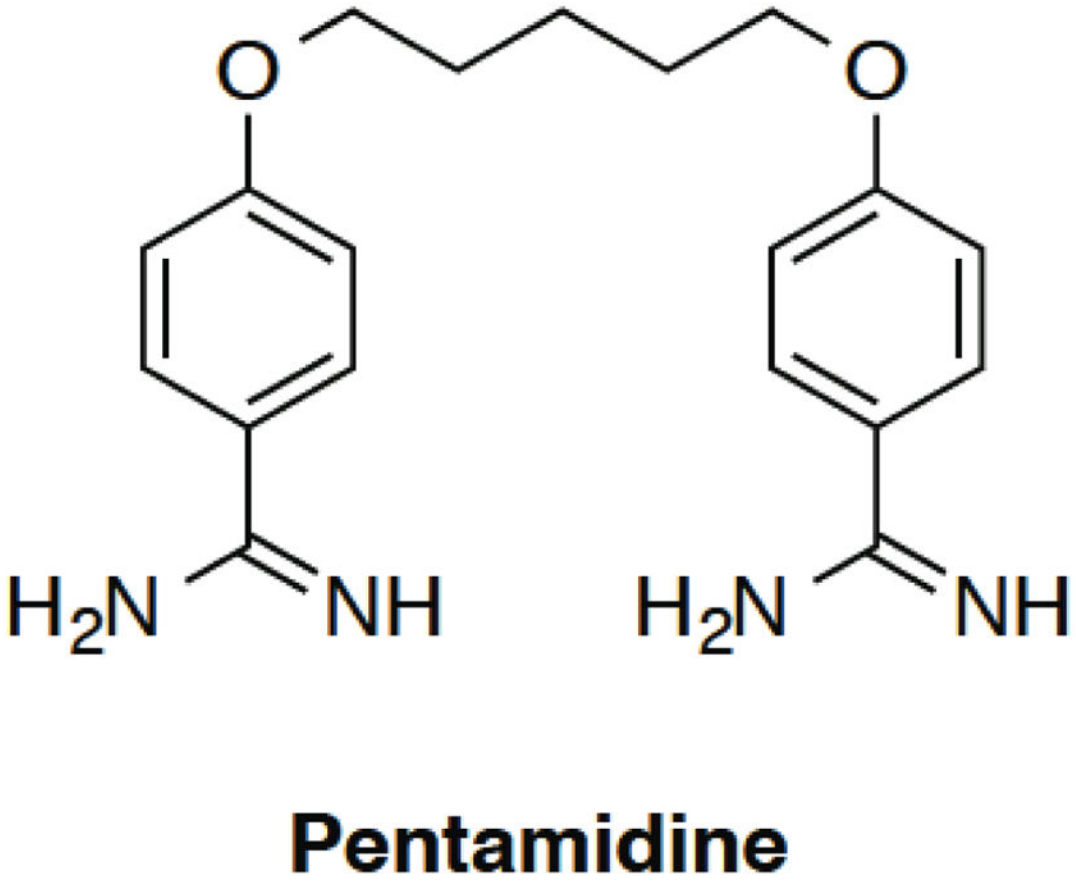


**Figure 1.**
Chemical structure of pentamidine.

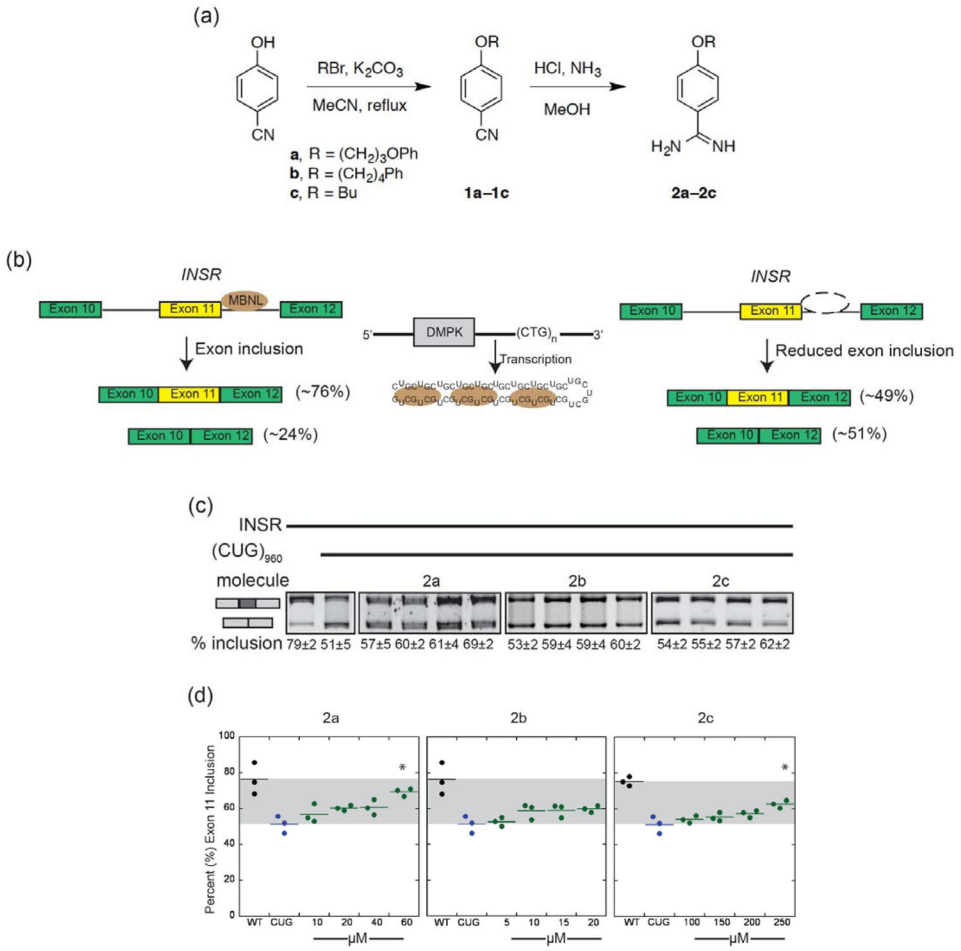


**Figure 2. SAR study of pentamidine derivatives**

**(a)** General synthetic schematic for pentamidine derivatives **2a–2c**.

**(b)** Schematic depicting the effect of CUG repeat RNA on the splicing of *INSR*. Percentages listed indicate percentage inclusion/exclusion of alternatively spliced exon 11, as quantified in a minigene transfection system.

**(c)** RT-PCR data of *INSR* splicing in cells incubated with increasing concentrations of compounds **2a–2c**. Results are depicted as average percentage of exon 11 inclusion ± standard deviation of three independent trials.

**(d)** Jitter plot representation of *INSR* splicing in cells treated with compounds **2a–2c**. Each point is one experiment and the line represents the average of all experiments for that condition (at least three for each concentration). Gray area denotes range between typical splicing and DM1-induced mis-splicing. Concentrations (in μM) are listed below. Asterisks indicate a significant difference between the treatment concentration and mis-splicing without compound.

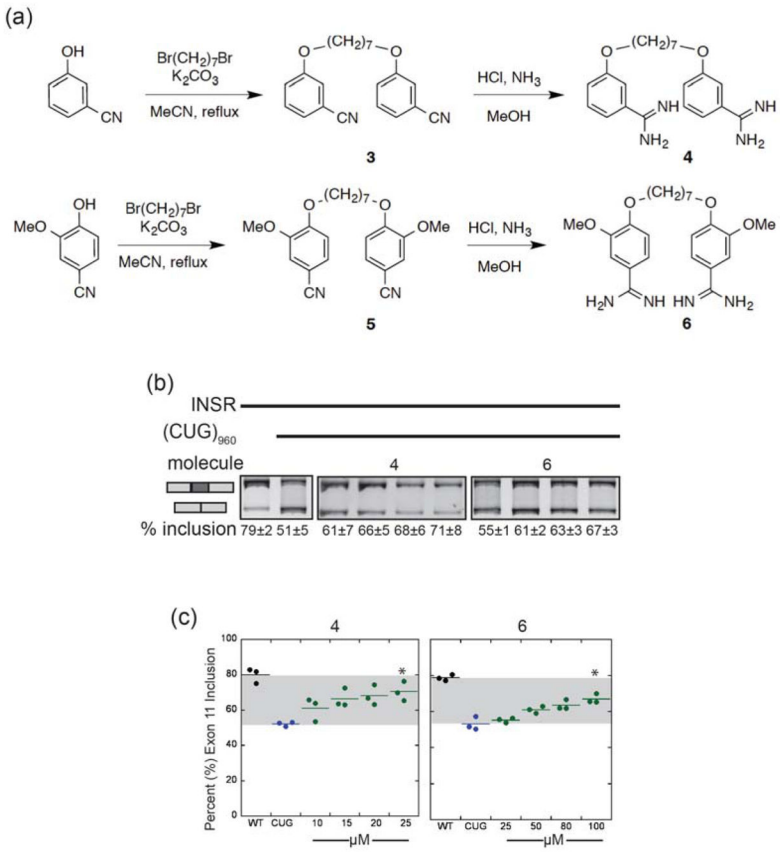


**Figure 3. Heptamidine analogues partially rescue mis-splicing of minigene reporters**

**(a)** General synthetic schematic for heptamidine derivatives **4** and **6**.

**(b)** RT-PCR data of *INSR* splicing in cells incubated with increasing concentrations of compounds **4** and **6**. Results are depicted as average percentage of exon 11 inclusion ± standard deviation of three independent trials.

**(c)** Jitter plot representation of *INSR* splicing in cells treated with compounds **4** and **6**. Asterisks indicate a significant difference between the treatment concentration and mis-splicing without compound.

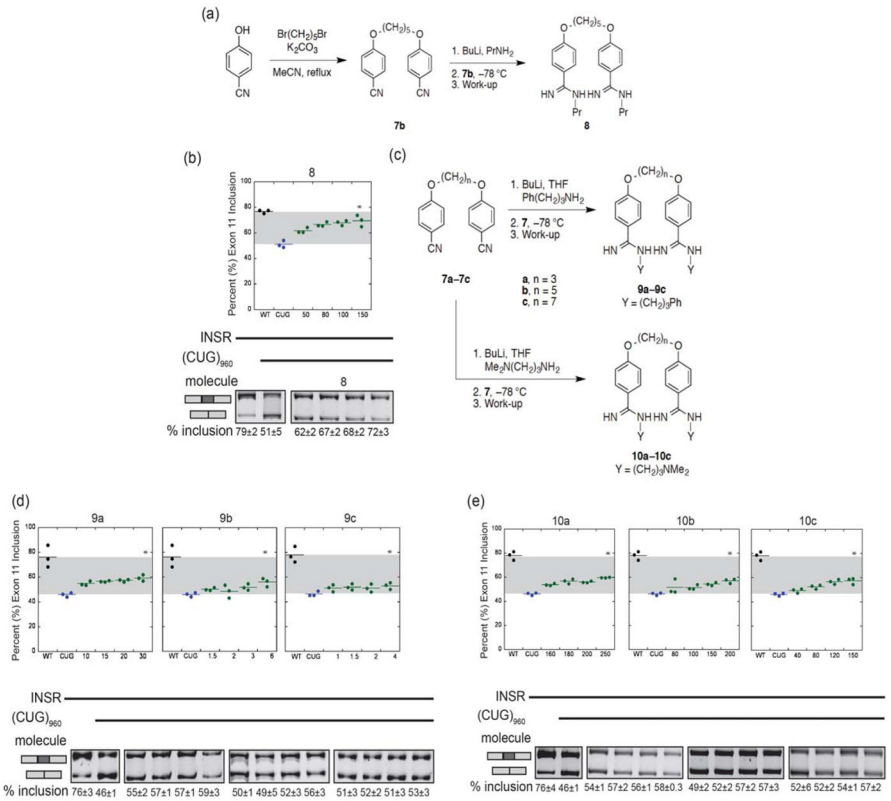


**Figure 4. N-substituted pentamidine derivatives demonstrate increased toxicity *in cellulo***

**(a)** General synthetic schematic for precursor to aminopropyl-substituted compounds.

**(b)** Jitter plot representation of *INSR* splicing in cells treated with compound **8**. Below, representative RT-PCR gel is demonstrated, with average percentage values (± standard deviation) listed per each condition. Asterisks indicate a significant difference between the treatment concentration and mis-splicing without compound.

**(c)** General synthetic schematic for phenyl-substituted (**9a–9c**) and N′N-dimethylaminopropyl-substituted (**10a–10c**) compounds.

**(d & e)** Jitter plot representation of *INSR* splicing in cells treated with compounds **9a–9c (d)** and **10a–10c (e)**. Below, representative RT-PCR gels are demonstrated, with average percentage values (± standard deviation) listed per each condition. Asterisks indicate a significant difference between the treatment concentration and mis-splicing without compound.

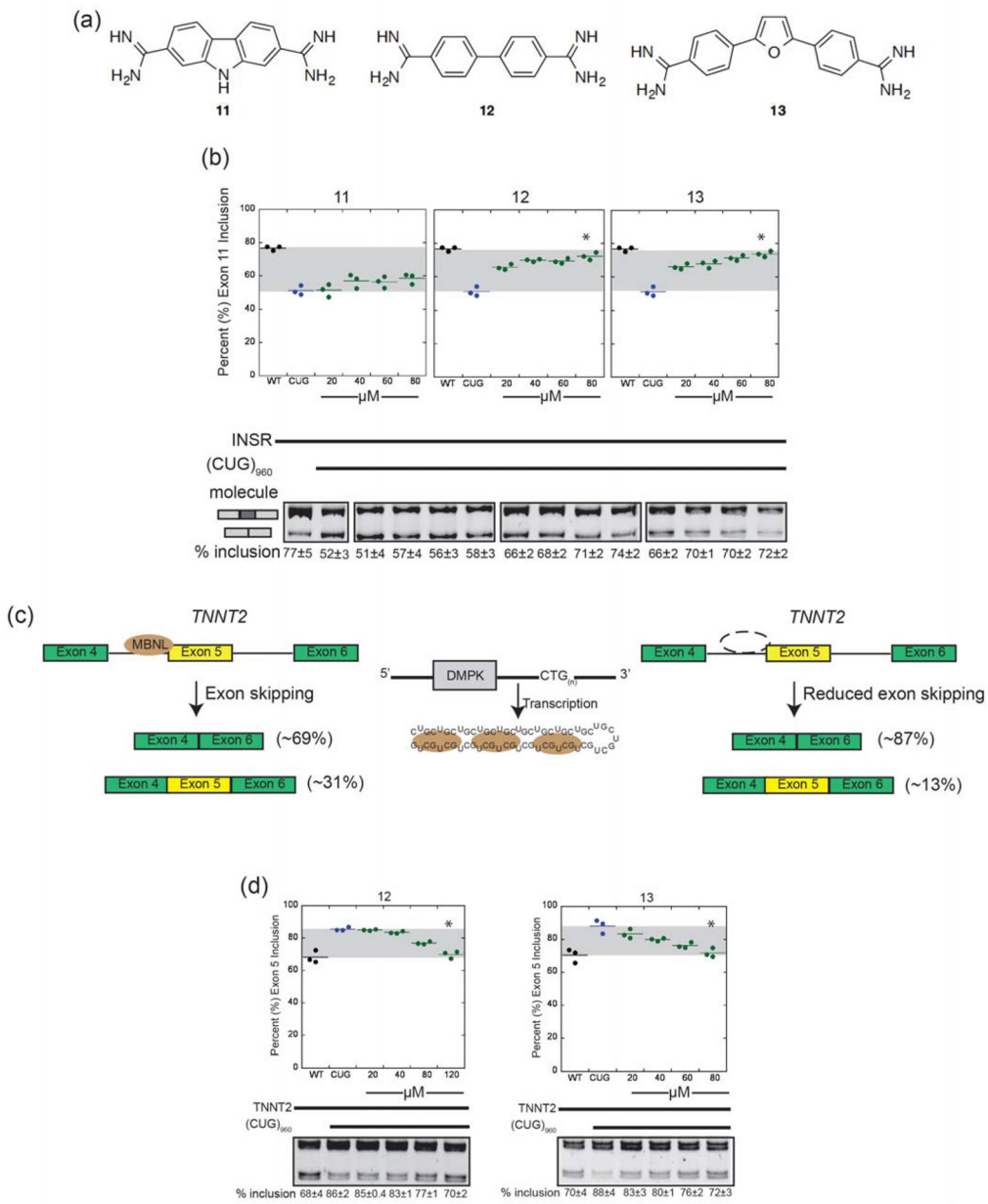


**Figure 5. Two conformationally-constrained diamidines (12 and 13) demonstrate decreased toxicity *in cellulo***

**(a)** General synthetic schematic for conformationally-constrained compounds **11–13**.

**(b)** Jitter plot representation of *INSR* splicing in cells treated with compounds **11–13**. Below, representative RT-PCR gels are demonstrated, with average percentage values (± standard deviation) listed per each condition. Asterisks indicate a significant difference between the treatment concentration and mis-splicing without compound.

**(c)** Schematic depicting the effect of CUG repeat RNA on the splicing of *TNNT2*. Percentages shown indicate percentage inclusion/exclusion of alternatively spliced exon 11, as quantified in a minigene transfection system.

**(d)** Jitter plot representation of *TNNT2* splicing in cells treated with compounds **12** and **13**. Below, representative RT-PCR gels are demonstrated, with average percentage values (± standard deviation) listed per each condition. Asterisks indicate a significant difference between the treatment concentration and mis-splicing without compound.

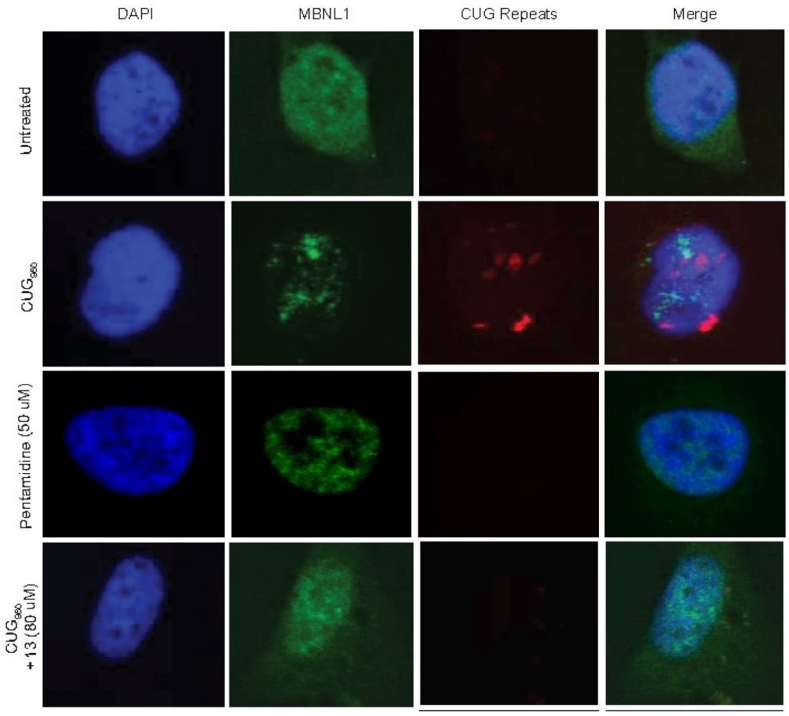


**Figure 6. Compound 13 reduces nuclear aggregation of MBNL1**

Compound **13** reduces ribonuclear foci and relieve MBNL1 sequestration. Top row: untreated HeLa cells, with MBNL1 localizing diffusely throughout the nucleus. Second row: Transfection of $CUG_{960}$ plasmid results in the formation of ribonuclear foci. Addition of 50 μM pentamidine (third row) or 80 μM compound **13** (fourth row) results in significant reduction of ribonuclear foci.

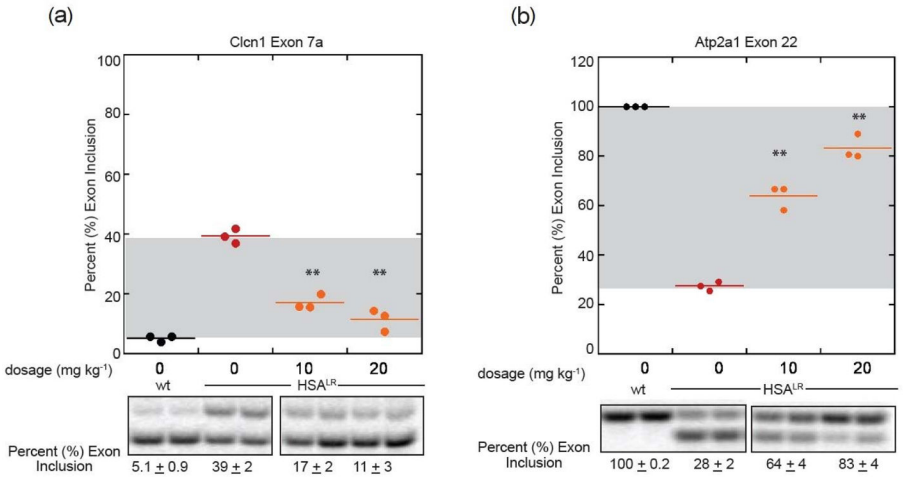


**Figure 7.**

Compound **13** rescues mis-splicing in a DM1 mouse model. a) Compound **13** was able to partially rescue the chloride channel endogenous event by 20 mg/kg for 7 d. b) Compound **13** was also able to partially rescue the sarcoplasmic calcium ATPase 1 endogenous event by 20 mg/kg for 7 d. No toxicity was observed over the concentration range tested. Each symbol represents the splicing outcome for quadriceps muscle of a single mouse. Gray area denotes range of splicing between wild type and DM mis-splicing patterns. Asterisks denote events that were significantly different from $HSA^{LR}$ mice.

**Table 1**

**Efficacy ($EC_{50}$) and cytotoxicity ($IC_{50}$) values for diamidine derivatives of pentamidine and heptamidine**

Asterisk indicated that $EC_{50}$ values are mathematically predicted, but where never reached experimentally due to toxicity. All values reported as +/− standard deviation.

| | $EC_{50}$ | $IC_{50}$ | $EC_{50}$:$IC_{50}$ |
|---|---|---|---|
| **Pentamidine** | 31 ± 2 | 64 ± 12 | 0.48 |
| **Heptamidine** | 9 ± 1 | 15 ± 0.46 | 0.60 |
| **4** | 14 ± 5.2 | 30 ± 4.9 | 0.47 |
| **6** | 75 ± 11 | 91 ± 8.4 | 0.82 |
| **8** | 70 ± 12 | 355 ± 45.1 | 0.20 |
| **9a** | 40* ± 9.3 | 13 ± 2.9 | 3.08 |
| **9b** | 10.5* ± 5.4 | 11 ± 1.6 | 0.95 |
| **9c** | 10.4* ± 2.9 | 5 ± 0.26 | 2.08 |
| **10a** | 366* ± 14.9 | 551 ± 35.4 | 0.66 |
| **10b** | 393* ± 94.2 | 414 ± 31.2 | 0.95 |
| **10c** | 256* 68.2 | 217 ± 16.2 | 1.18 |
| **11** | 125* 54.4 | 134 ± 55.8 | 0.93 |
| **12** | 31 ± 4 | 210 ± 19.3 | 0.15 |
| **13** | 30 ±4 | N/A | N/A |